Journal of Asian Earth Sciences 116 (2016) 222–231

Contents lists available at ScienceDirect

Journal of Asian Earth Sciences

journal homepage: www.elsevier.com/locate/jseaes

Diachronous seawater retreat from the southwestern margin of the Tarim Basin in the late Eocene

Jimin Sun [a,b,*], Brian F. Windley [c], Zhiliang Zhang [a], Bihong Fu [d], Shihu Li [a]

[a] Key Laboratory of Cenozoic Geology and Environment, Institute of Geology and Geophysics, Chinese Academy of Sciences, Beijing, China
[b] CAS Center for Excellence in Tibetan Plateau Earth Sciences, China
[c] Department of Geology, University of Leicester, Leicester LEI 7RH, UK
[d] Institute of Remote Sensing and Digital Earth, Chinese Academy of Sciences, Beijing, China

ARTICLE INFO

Article history:
Received 18 August 2015
Received in revised form 23 November 2015
Accepted 24 November 2015
Available online 24 November 2015

Keywords:
Tarim Basin
Pamir
Cenozoic
Neotethys
Diachronous sea retreat

ABSTRACT

In contrast to the present hyper-arid inland basin surrounded by the high mountains of Central Asia, the western Tarim Basin was once connected with the Tajik Basin at least in the late Eocene, when an epicontinental sea extended from the western Tarim Basin to Europe. Western Tarim is a key site for studying the retreat of seawater, which was likely caused by the northward indentation of the Pamir arc and facilitated by the climatic cooling and eustatic sea level change in the Cenozoic. Here we present a new magnetostratigraphic record from the Tarim Basin that provides evidence of diachronous seawater retreat from its southwestern margin. We studied about 1360 m of well-exposed Eocene–Oligocene strata at Keliyang in the folded foreland of the West Kunlun orogen. Until now, the age of the strata has only been minimally constrained by the presence of late mid-Eocene marine fossils. Our biostratigraphic and magnetostratigraphic results demonstrate that the age of the sedimentary sequence ranges from ~46 Ma to ~26 Ma (mid-Eocene to late-Oligocene) and the seawater retreat at Keliyang took place at ~40 Ma. Considering the stepwise northward indentation and uplift of the Pamir orogen, together with the other previous results, we propose that seawater retreat from the southwestern margin of the Tarim Basin was diachronous in the late Eocene ranging from 47 Ma to 40 Ma. The regional indentation, uplift and erosion of the Pamir orogen played the dominant and important role in controlling the seawater retreat from the southwestern margin of the Tarim Basin.

1. Introduction

The Tarim Basin is the largest inland basin in northwestern China occupying an area of about 530,000 km^2. It is bordered by the Tian Shan Range to the north, the Pamir Plateau to the west, and the Kunlun range to the south (Fig. 1). At present, this basin is mainly covered by the large Taklimakan Desert that developed at the end of Miocene (Sun and Liu, 2006; Chang et al., 2012; Liu et al., 2014; Sun et al., 2015). However, during the early Paleogene, the western part of the basin was occupied by a shallow epicontinental sea (referred to as the Tarim Sea) that was an eastern branch of the Neotethys Ocean (e.g., Rögl, 1999; Popov et al., 2004, 2006; Vasiliev et al., 2004; Schulz et al., 2005; Piller et al., 2007; Bosboom et al., 2011, 2014a, 2014b; Bershaw et al., 2012; Sun and Jiang, 2013; Wang et al., 2014).

The evolution of the Tarim Sea is important for understanding the Cenozoic tectonics of the western Himalayan–Tibetan orogen, because the seawater retreat from different parts of the Tarim Basin was closely linked to the northward indentation of the Pamir Plateau and by eustatic sea level changes forced by Cenozoic cooling (Bosboom et al., 2014a; Sun and Jiang, 2013).

However, the timing of the final seawater retreat either from the southwestern margin or the whole Tarim Basin is controversial. Guo and Ding (2002) proposed a mid-Miocene sea retreat depending only on biostratigraphic correlations, and without any precise age controls. Ritts et al. (2008) argued that a connection to open marine waters still existed in the southern Tarim Basin at 15 Ma; however, their marine foraminifera were reported from thin reddish mudstones interbedded in a thick Miocene conglomerate. Although the age of the foraminifera could be limited to the mid-Miocene (Ritts et al., 2008), such microfossils could easily have been re-transported for long-distances by prevailing westerly winds from the remote upwind regions (far beyond the western margin of the Tarim Basin) during the retreat of Paratethys. The

* Corresponding author at: Key Laboratory of Cenozoic Geology and Environment, Institute of Geology and Geophysics, Chinese Academy of Sciences, Beijing, China.
E-mail address: jmsun@mail.igcas.ac.cn (J. Sun).

http://dx.doi.org/10.1016/j.jseaes.2015.11.020
1367-9120/

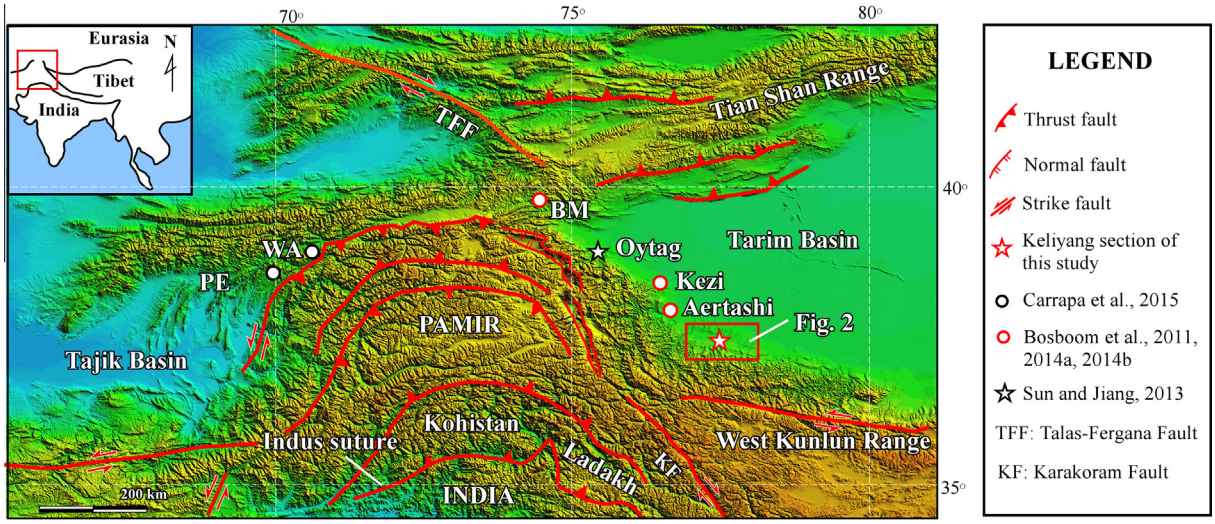

Fig. 1. Digital Elevation Map of the Pamir salient showing major suture zones, tectonic terranes, and the location of the sections mentioned in the text. Tectonic terranes and major Cenozoic structures are mainly after Burtman and Molnar (1993), Yin et al. (2002), Robinson et al. (2004), Cowgill (2010), and Fu et al. (2010).

mixing of marine microfossils of different ages including the mid-Miocene foraminifera together with corroded, reworked specimens of Jurassic and Late Cretaceous nannofossils in the same layer (as described by Ritts et al., 2008) possibly implies reworking and re-transportation. Wang et al. (2014) suggested that seawater retreat from the western Tarim Basin was at 34 Ma; however, their chronology was mainly based on previous biostratigraphy without high-resolution magnetostratigraphy. Bosboom et al. (2011) proposed that the sea retreated from the southwestern Tarim Basin at 37 Ma based on biostratigraphy (for the marine fossils of the Aertashi and the Kezi sections, see Fig. 1 for locations), but this age was corrected to 41 Ma after they performed a high-resolution magnetostratigraphic analysis of the Aertashi strata (Bosboom et al., 2014a, 2014b). Sun and Jiang (2013) reported that seawater retreat was at 47 Ma from their study of the Oytag section that is located in the eastern foreland of the Pamir. Recently, Carrapa et al. (2015) carried out a multidisciplinary study in the eastern Tajik Basin about 400 km to the west of the Tarim Basin, which included biostratigraphy, U–Pb geochronology of detrital zircons (the youngest ages limit the maximum deposition age of the sediments), and geochronology of a Cenozoic volcanic ash layer, which provided a robust age of 39 Ma for the retreat of sea water from the eastern Tajik Basin. The above contrasting views necessitate new reliable data to define the precise time of seawater retreat from different parts of the Tarim Basin.

This study focuses on Paleogene marine–terrestrial sediments at Keliyang that is situated in the southwest Tarim Basin. We aim to provide new biostratigrahic and high-resolution magnetostratipraphic data to constrain the timing and history of seawater retreat at this site. Finally we present a new model, integrated with relevant published data, to explain the spatially non-isochronous seawater retreat from the southwestern margin of the Tarim Basin on a tectonic time scale (millions of years).

2. Geological setting

The Western Kunlun Range (Fig. 1), one of the highest and the most actively eroding mountain belts in Asia, is located on the northern margin of the Tibetan Plateau, the uplift being closely linked to the India–Eurasia convergence in the Cenozoic (Tapponnier and Molnar, 1979; Yin and Harrison, 2000; Yin et al., 2002; Wang et al., 2003; Xiao et al., 2003). In its northern foreland there are spectacular fold-and-thrust belts parallel to the main mountain range, where the Kunlun North Frontal Thrust marks the boundary between the Proterozoic–Paleozoic–early Mesozoic orogen to the south (Xiao et al., 2005) and the Cenozoic foreland basin to the north (Fig. 2). Cenozoic clastic material eroded off the mountain belt has been accumulated in the North Pamir-Kunlun foreland. These sediments, which are up to ~8–10 km thick (Li et al., 1996), thin progressively northwards from the West Kunlun orogen toward the Tarim Basin, and thus provide important information about the formation of the northward-propagating fold-and-thrust belts, the changes of sedimentary facies related to the topographic evolution and the northward-propagating deposition, and the timing of the seawater retreat from different parts of the Tarim Basin.

Near Keliyang (Fig. 2) the foreland basin contains Paleogene to Neogene deposits, but only the Paleogene strata are sufficiently well-exposed to provide adequate sampling. All the Paleogene strata are structurally overturned with steep dips between 75° and 85° to the southeast (Fig. 3). Previous research on this stratigraphic section has mostly focused on sedimentology and biostratigraphy (e.g., Lan and Wei, 1995; Jin et al., 2003; Bosboom et al., 2014a).

At Keliyang the ~1360 m-thick Paleogene strata are divided into three units (Figs. 3 and 4). The lowest is an ~80 m-thick terrestrial 'red bed' that mainly consists of reddish sandstone with two intercalated conglomerate beds (Fig. 4a and b), sedimentary facies indicates a fluvial environment.

Above this terrestrial 'red bed', there is a 270 m-thick unit that consists of interbedded marine and continental facies (Fig. 3) bearing marine bivalves, dinoflagellates, ostracods, and foraminifera (He, 1991; Pan et al., 1991; Zhong, 1992; Lan and Wei, 1995; Yang et al., 1995; Bosboom et al., 2014a). The lithology of this unit is characterized by marine dolomitic limestone–packstone, intertidal grey mudstone–sandstone, tidal sabkha evaporite gypsum, as well as intercalated terrestrial mudstones (Fig. 4c, left side), suggesting that sedimentary conditions fluctuated between shallow marine and terrestrial (Fig. 4d, e).

Above the interbedded marine and continental facies, there is a 1100 m thick terrestrial sequence mainly consists of alternating reddish to reddish-brown, laminated mudstones and sandstones (Fig. 4c, right part), representing a fluvial-lacustrine sedimentary facies.

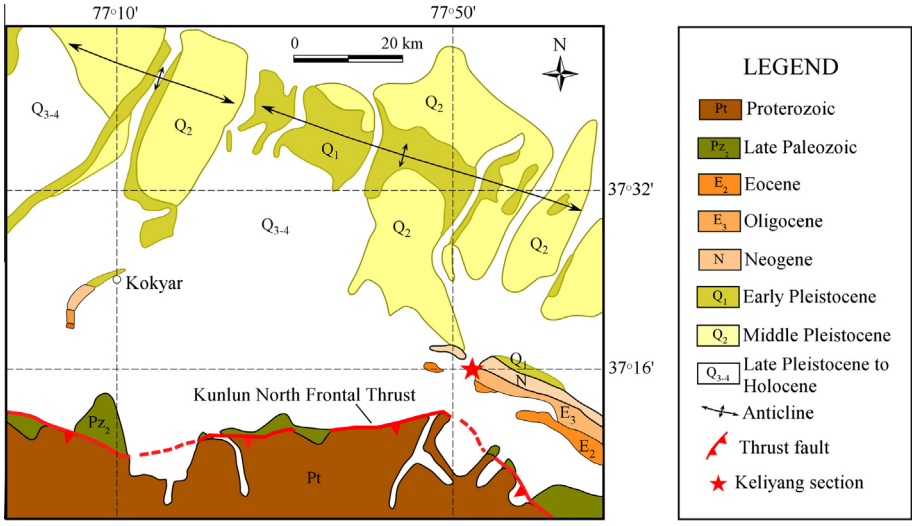

Fig. 2. Geological sketch map of the study region showing the location of the Keliyang section (modified after Cheng et al., 2011), and the axial trace of the folded foreland basin sediments.

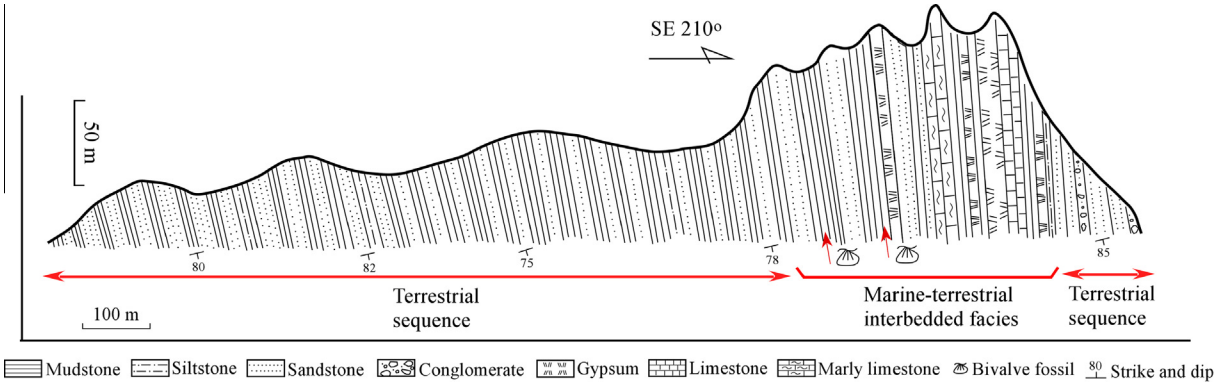

Fig. 3. Cross-section of the Keliyang section showing Eocene to Oligocene strata. Red arrows indicate the positions of the two marine fossil zones. (For interpretation of the references to color in this figure legend, the reader is referred to the web version of this article.)

3. Material and methods

During two field expeditions in 2005 and 2015, 660 oriented specimens were cored with a portable gasoline-powered drilling from 330 sites (two samples were drilled at every site). Orientations were measured with an inclinometer to measure the inclination (dip) of the core axis, and a magnetic compass (Suunto MC-2) to determine the core axis azimuth. The accuracy of such an orientation is about ±2°.

All samples were subjected to stepwise thermal demagnetization with a Magnetic Measurement Thermal Demagnetizer (MMTD Model 80). In general, thermal demagnetization intervals were 25–50 °C below 610 °C and 10–20 °C above 610 °C. Magnetic remanence was measured with a 2G-760 U-channel, three-axis, cryogenic magnetometer housed in field-free space (<300 nT) at the Paleomagnetism and Geochronology Laboratory in the Institute of Geology and Geophysics, Chinese Academy of Sciences (IGGCAS) in Beijing. The characteristic directions of magnetization were determined by least squares fitting (Kirschvink, 1980) with selected demagnetization data points (minimum of three, but typically four to eight), and directions were analyzed using Fisher statistics (Fisher, 1953).

Temperature dependence of low-field magnetic susceptibility was also measured by cycling through the range of room temperature to 700 °C in argon, using a KLY-3 Kappabridge magnetic susceptibility meter equipped with a high-temperature furnace at IGGCAS. The sample holder and thermocouple contributions to magnetic susceptibility were subtracted.

4. Results

4.1. Rock magnetic experimental results

Rock magnetic studies were undertaken in order to determine the mineralogy and morphology of the magnetic components of these rocks. All measured samples show an irreversible behavior of low-field magnetic susceptibility versus temperature (Fig. 5). Analysis of the heating curves demonstrates noticeable decreases of the magnetic susceptibility around temperatures of 580 °C and 680 °C (Fig. 5), indicating the presence of magnetite and hematite, respectively. Because the bulk susceptibility of magnetite is ~1000 times greater than that of most rock materials (Collinson, 1983), this thermomagnetic behavior suggests that the magnetic minerals are dominated by hematite with magnetite as a subordinate ferromagnet.

4.2. Demagnetization

We analyzed 330 oriented samples of which we successfully isolated the characteristic remanent magnetization (ChRM) in

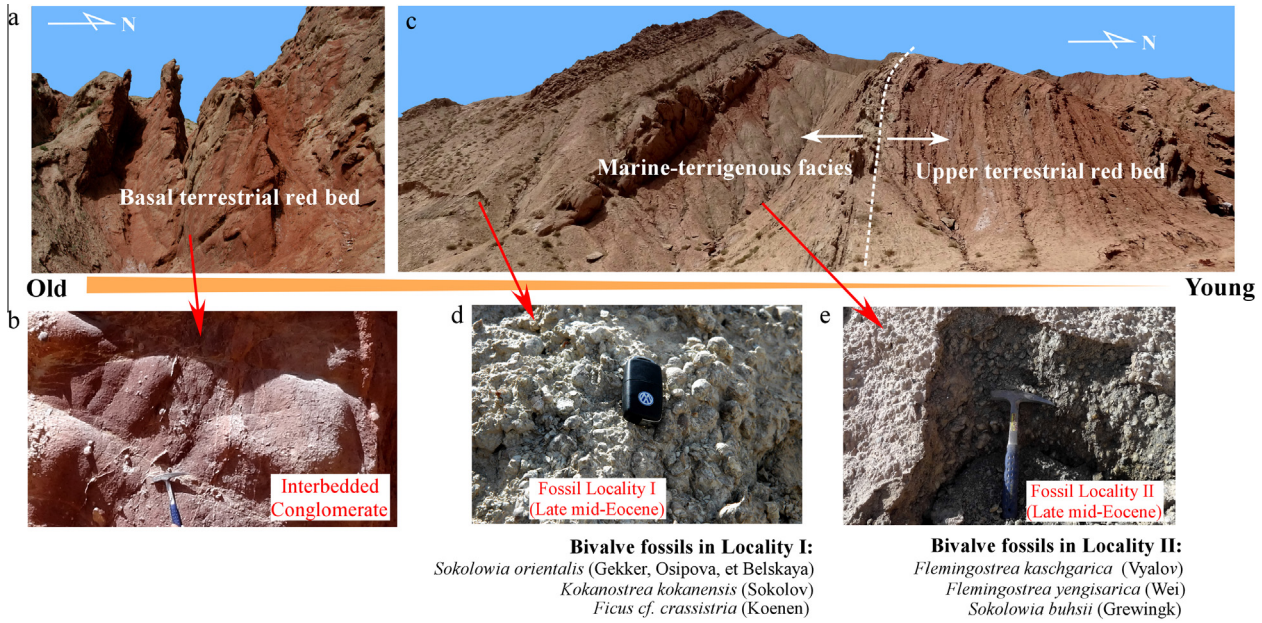

Fig. 4. Photos showing Paleogene sediments at Keliyang. (a) The lowest terrestrial red bed. (b) Intercalated conglomerates within the lowest red bed. (c) Boundary between the marine–terrestrial interbedded strata and the upper terrestrial reddish mudstone/sandstone alternations. (d) Marine bivalve fossils in Fossil Locality I. (e) Marine bivalves in Fossil Locality II. For detailed stratigraphic section see Fig. 3. (For interpretation of the references to color in this figure legend, the reader is referred to the web version of this article.)

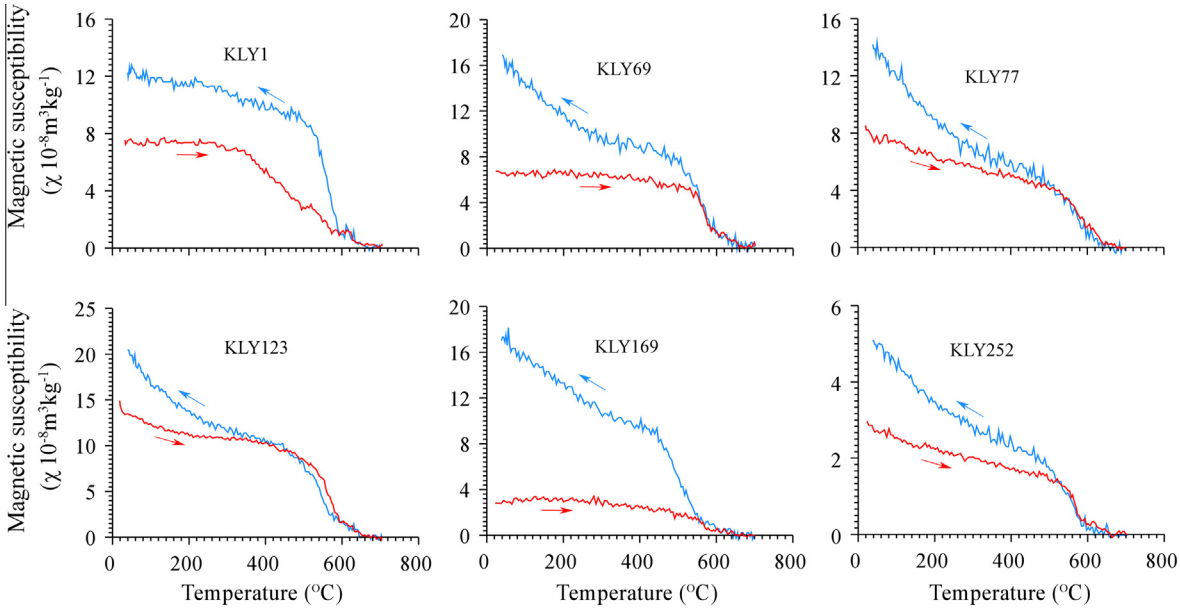

Fig. 5. Temperature dependence of magnetic susceptibility (k–T curves) of representative samples from different levels of the section. All spectra were determined by heating from room temperature to 700 °C and then cooling to room temperature in an argon gas atmosphere. The arrows indicate the directions of temperature change (red: heating; blue: cooling). All the selected samples manifest sharp drops at temperatures of ~550–580 °C (magnetite) and of ~680 °C (hematite) in the heating curves. (For interpretation of the references to color in this figure legend, the reader is referred to the web version of this article.)

274 samples after removal of one or two soft secondary components of magnetization. Representative demagnetization diagrams are shown in Fig. 6. The majority of the samples displayed a two-component magnetization (Fig. 6a–c and e–f), consisting of a low-temperature component, and a dual polarity characteristic remanent magnetization. The low-temperature component is similar to the local present-day normal polarity, and may relate to an overprint direction of recent origin; it was removed after moderate heating to 250–350 °C. Above this temperature, a characteristic remanent magnetization of either normal or reversed polarity was identified. In most samples, the ChRM shows maximum unblocking temperatures ranging from 550 °C to 680 °C for the red-colored siltstones and sandstones, which suggests that it is carried by the iron oxides magnetite and haematite, being consistent with the rock magnetic results revealed by the temperature dependence of magnetic susceptibility. Occasionally, three magnetic components were isolated (Fig. 6d) including a subrecent normal polarity overprint at low temperature (below 300–350 °C), an intermediate component with unblocking temperatures ranging from 350 °C to 500 °C, and a third, dual-polarity

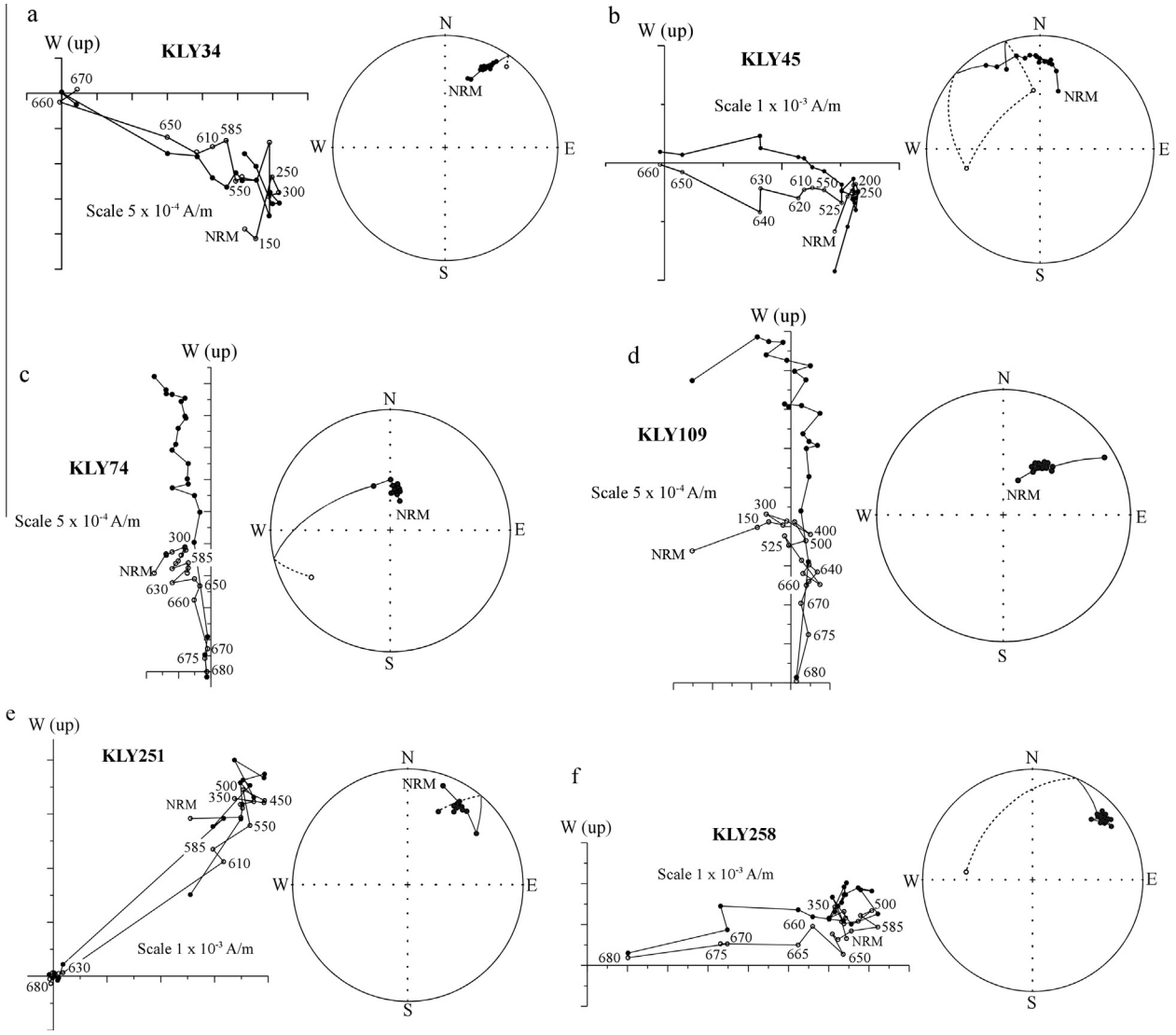

Fig. 6. Six representative orthogonal vector plots and equal-area stereographic projections for specimens from the Keliyang section. In orthogonal projection, solid (open) symbols refer to the projection on the horizontal (vertical) plane. Full (open) circles in stereographic plots represent projections onto the lower (upper) hemisphere. Demagnetization steps are in °C, and NRM is the natural remanent magnetization. The data are shown in tilt-corrected coordinates.

component above 500 °C (Fig. 6d) for this reddish mudstone specimen. It is difficult to assign a magnetization age for the intermediate component, however, because its occurrence is limited to a few sites; its origin is probably related to an early post-depositional magnetization and not to a remagnetization event. We did not perform a fold test because there are only minor variations in structural attitude.

4.3. Reversal test

The specimens' ChRM directional data were analyzed for a reversal test by using the formulation of McFadden and McElhinny (1990), in order to test for antiparallel field orientations. In the illustrations of the reversal test (Fig. 7a and b), the mean of the normal-polarity sites is $Dec_N = 11.5°$, $Inc_N = 40.7°$, $\kappa = 7.7$, $\alpha_{95} = 4.3°$; whereas the mean of the reversed-polarity sites is $Dec_R = 190.4°$, $Inc_R = -35.1°$, $\kappa = 6.0$, $\alpha_{95} = 6.0°$ after tilt-correction. When the antipode of the reversed-polarity mean is compared with the normal-polarity mean, passing a reversal test with A classification (angular difference between the mean directions of normal and reversed polarities is 5.6°, which is smaller than the critical value of 7.81°). The result suggests that the paleomagnetic ChRM directions isolated from the rocks relate to a single component of magnetization, and are not contaminated by other components.

4.4. Biostratigraphy

Many earlier biostratigraphic studies at this site and other equivalent locations in the western Tarim Basin reported abundant marine fossils and skeletal fragments of bivalves, echinoids, bryozoans, foraminifera, gastropods, crustaceans, ostracods, and calcareous algae in carbonates and mudstones (He, 1991; Pan et al., 1991; Zhong, 1992; Lan and Wei, 1995; Yang et al., 1995; Bosboom et al., 2014a). During our fieldwork we also discovered two fossil localities (I and II) in greyish green mudstones intercalated within the marine–terrestrial interbedded facies (Fig. 4). All the fossils were identified by Xiu Lan, who carried out the pioneering work in the Tarim Basin (Lan and Wei, 1995). Locality I contains marine bivalve fossils of *Sokolowia orientalis* (Gekker, Osipova, et Belskaya), *Kokanostrea kokanensis* (Sokolov), and *Ficus cf. crassistria* (Koenen). Locality II contains other marine bivalve fossils of *Flemingostrea kaschgarica* (Vyalov), *Flemingostrea yengisarica* (Wei),

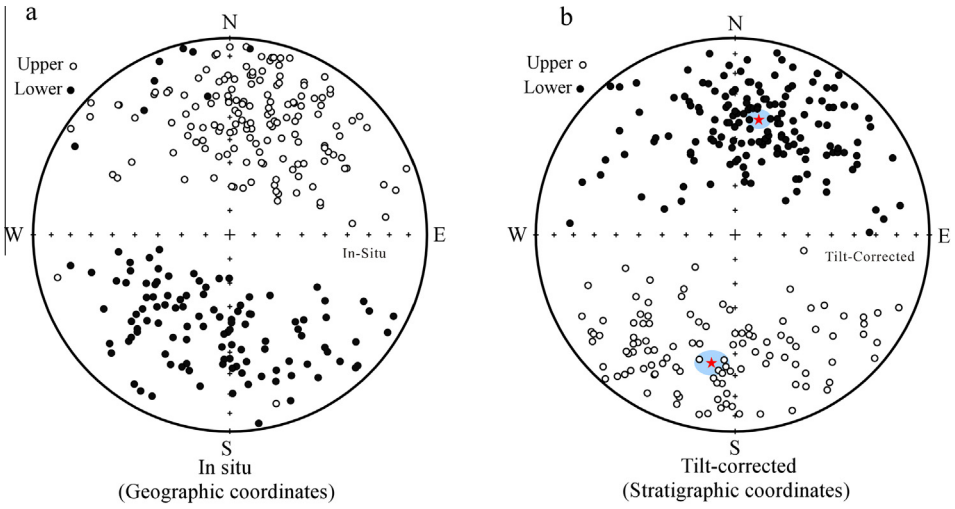

Fig. 7. Equal area projections of ChRM directions before (a) and after (b) tilt-correction. These data define an A-class reversal test (for details see the text) at a 95% confidence level. The solid and open circles represent lower hemisphere and upper hemisphere projections respectively. The red stars represent the mean directions after tilt-correction, and the blue areas indicate the 95% confidence limit of the mean directions. (For interpretation of the references to color in this figure legend, the reader is referred to the web version of this article.)

and *Sokolowia buhsii* (Grewingk) (Fig. 4); *Sokolowia buhsii* was also reported by Bosboom et al. (2014a) at Keliyang. According to Lan and Wei (1995), these fossils are late mid-Eocene in age and belong to the Wulagen Formation.

4.5. Magnetostratigraphy

Magnetostratigraphy is a useful tool to provide chronology of sediments based on the correlation of a measured magnetic polarity column to a standard Geomagnetic Polarity Time Scale (GPTS) (Cande and Kent, 1995, CK95), when polarity changes are well dated via independent methods (radiogenic ages and astronomical constraints). However, because the polarity of a stratum can only be normal or reversed, variations in the sedimentation rate can cause the thickness of a given polarity zone to vary from one area to another. This presents the problem of how to correlate the measured polarity column with the GPTS; this is especially the case in active fold-and-thrust foreland basins, where there are likely sedimentary hiatuses due to faulting or denudation. Therefore, it is helpful to have either the isotopic age of a basalt/tuff and/or the biostratigraphic age of a sediment, although potential problems may still exist due to unsteady sedimentation rates or the presence of large hiatuses.

The declinations and inclinations obtained for the characteristic remanent magnetization of our specimens were used to calculate the virtual geomagnetic pole (VGP) latitude, which yields a magnetic polarity sequence (Fig. 8). In the Keliyang section, two late mid-Eocene marine bivalve fossil localities occur in the lower part/unit of the section. Based on the biostratigraphic age control, we can correlate the measured magnetostratigraphy with the GPTS of CK95 in order to generate high-resolution chronology.

The most prominent feature of this magnetostratigraphy is the relatively long normal polarities (N5 to N9) punctuated by several relatively short reversal polarities (R4–R8), which can be correlated with the dominant normal polarities of C18n.2n to C16n.2n of the GPTS CK95 (Fig. 8). It is worthy noting that the distinct long normal polarity of N9 is mostly due to its large sampling intervals, which have led to the omission of several short reversal magnetic chrons. The above correlation yields an age of ~40 Ma for the marine fossils, which is coherent with the biostratigraphic data of a late mid-Eocene age (Lan and Wei, 1995). Therefore, we reject other alternative correlations. Above and below this interval, the correlation becomes easier, because the upper part of the magnetic polarity sequence from N10 to N18 perfectly matches C16n.1n to C8n.1n of GPTS CK95, whereas the lower part from R1 to R4 correlates with C20r to C18r (Fig. 8). Therefore, the magnetozones of the Keliyang section correlate with the polarity chrons from the topmost C22n to the end of C8n.1n of GPTS CK95; i.e. they cover an age range from ~46 Ma to ~26 Ma (Fig. 8).

5. Discussion

5.1. Diachronous seawater retreat from the southwestern margin of the Tarim Basin during the late Eocene

At present, the Pamir orogen breaks the link between the Tarim Basin and the other westerly depressions (e.g., the Tajik Basin) once occupied by seawater of Neotethys (Fig. 1), when the Paleogene landform was quite different from the present configuration. An increasing body of evidence demonstrates that the Cenozoic northward indentation of the Pamir orogen was an integral part of the India-Eurasia collision (Molnar and Tapponnier, 1975; Searle et al., 1999; Waldhör et al., 2001; Robinson et al., 2004, 2007, 2012; Schwab et al., 2004; Cowgill, 2010; Searle, 2011; Bershaw et al., 2012; Replumaz et al., 2013, 2014) (Fig. 1), and that the Cenozoic crustal shortening in the Pamir orogen was up to 300–400 km (Burtman and Molnar, 1993; Burtman, 2000). This accounts for the prominent northward orocline of the Pamir salient at the western end of the Himalayan–Tibetan orogen. Before the northward Pamir indentation, the southern Tian Shan orogen and the Pamir orogen were at least 300 km apart (Burtman and Molnar, 1993) separated by an epicontinental sea, which enabled an exchange of seawater between the Tarim Sea and the eastern branch of the Neotethys Ocean during the late Cretaceous and early Paleogene (e.g., He, 1991; Pan et al., 1991; Zhong, 1992; Lan and Wei, 1995; Yang et al., 1995; Bosboom et al., 2011, 2014a, 2014b; Sun and Jiang, 2013; Carrapa et al., 2015). The presence of this oceanic gateway is confirmed by several sites with early Cenozoic marine records in the western Tarim Basin (Fig. 9a).

The question that we now wish to address is: when did the seawater finally retreat from different parts of the Tarim Basin? One thing is certain: the timing of the final sea water migration and retreat must have been spatially diachronous. Firstly, in the

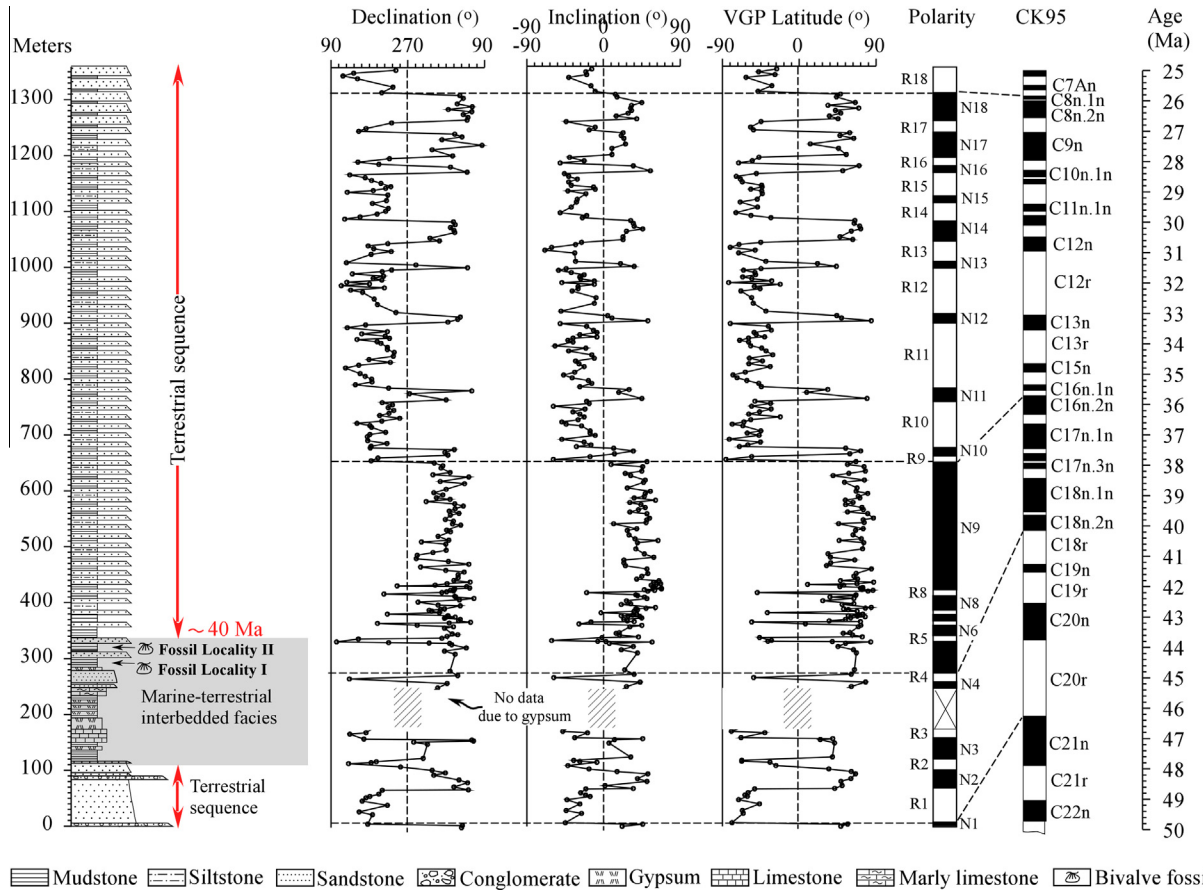

Fig. 8. Magnetostratigraphy of the Keliyang section. Magnetic polarity is compared with the standard geomagnetic polarity time scales (GPTS). CK95: GPTS of Cande and Kent (1995).

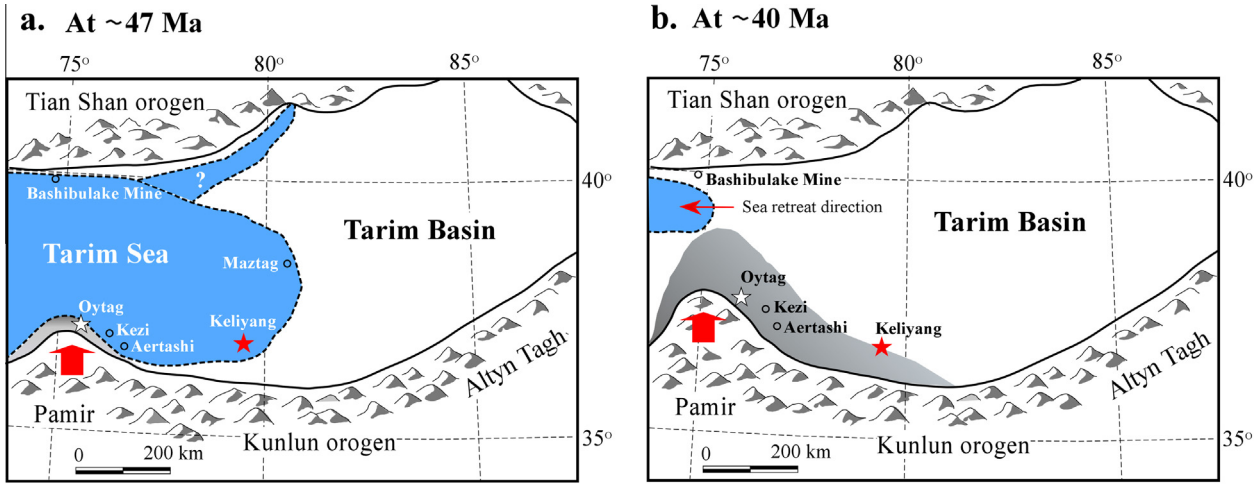

Fig. 9. Schematic maps showing the diachronous seawater retreat during the middle to late Eocene. (a) Early seawater retreat (~47 Ma) at Oytag on the eastern edge of the Pamir orogen was in response to the uplift and northward indentation of the Pamir salient; a sea still existed at Kezi, Aertashi, the Bashibulake Mine (Bosboom et al., 2014a, 2014b), Maztag (Lan and Wei, 1995) and at Keliyang. (b) Later seawater retreat (~40 Ma) in the southwestern margin of the Tarim Basin. Solid arrows indicate the indentation direction of the Pamir salient.

western Tarim Basin many authors (e.g., He, 1991; Pan et al., 1991; Zhong, 1992; Lan and Wei, 1995; Yang et al., 1995) reported extensive marine deposits, which indicated the presence of a vast shallow sea at least 300 km wide (north–south) and 400 km long (Fig. 9a). The retreat of seawater from such a large area of the Tarim Basin could not have been isochronous on tectonic time scales. Secondly, during the Cenozoic, the northern Pamir had indented northwards for ~300 km relative to stable Eurasia (Burtman and Molnar, 1993), and geophysical data indicate that the Indian plate underthrust the Eurasian crust in the Pamir to a depth of 300–500 km (Negredo et al., 2007; Burtman, 2013). Due to the oblique subduction of the Indian lithosphere underneath the Pamir (Tapponnier et al., 2001), it is likely that the uplift and the northward indentation of the Pamir salient was not

synchronous along and across this wide regional collision zone. Low-temperature thermochronology from the interior and margins of the Pamir Plateau suggests that exhumation and shortening propagated northward (e.g., Sobel and Dumitru, 1997; Amidon and Hynek, 2010; Thiede et al., 2013; Cao et al., 2013; Thompson et al., 2015). In response to this northward migration of indentation and uplift of the Pamir arc, the seawater retreat from the southwestern margin of the Tarim Basin should likewise have been diachronous on tectonic time scales.

Sun and Jiang (2013) demonstrated that seawater retreated at ~47 Ma from the Oytag section of the southwestern Tarim Basin (Fig. 9a); this is the earliest time of sea retreat recorded in the region compared with other studies (e.g., Guo and Ding, 2002; Ritts et al., 2008; Bosboom et al., 2011, 2014a, 2014b; Wang et al., 2014). This section is located on the northeastern margin of the Pamir syntaxis, and thus was particularly responsive to the advancing front of the Pamir salient resulting in early seawater retreat at Oytag (Fig. 9a). It should be noted that, although the northern margin of the Pamir had advanced northwards more than 300 km since Paleogene time (Burtman and Molnar, 1993), such a major northward displacement did not take place in the eastern part of West Kunlun and Altyn orogens, which can explain the existence of sea water ca. ~47 Ma at Keliyang (Fig. 9a).

According to correlations between the measured magnetostratigraphy and the GPTS, the uppermost marine strata in the Keliyang section have an age of ~40 Ma (Fig. 8). Therefore, our results demonstrate that seawater retreat at Keliyang was at ~40 Ma (Fig. 9b), which is later than at Oytag.

It is important to stress that Bosboom et al. (2014a, 2014b) reported that seawater retreat from the Aertashi, Kezi, and Bushibulake Mine sections were at about 41 Ma. Although they also thought that the transition from marine to terrestrial at Keliyang was at 41 Ma, they did not have magnetostratigraphic age control for this section, which had mainly been based on the biostratigraphic correlation with the well-dated Aertashi section (Bosboom et al., 2014a). Considering the uncertainties of magnetostratigraphic correlations, our results at Keliyang are comparable with those of Bosboom et al. (2014a, 2014b).

Additionally, Carrapa et al. (2015) demonstrated that sea water retreat from the eastern edge of the Tajik Basin was at 39 Ma. Because the Tarim Basin is located to the east of the Tajik Basin, the westward retreat of the sea must have been no later than in the Tajik Basin. According to our results, together with the evidence of Bosboom et al. (2014a, 2014b) and Carrapa et al. (2015), we suggest that the sea water retreat in the southwestern margin of the Tarim Basin was diachronous ranging from 47 Ma to 40 Ma, earlier at Oytag (due to the shorter distance to the Pamir orogen), and later at Keliyang (Fig. 9b).

5.2. Forcing mechanism for the diachronous seawater retreat in the southwestern margin of the Tarim Basin

Located at the western end of the Himalayan–Tibetan orogen, the Pamir salient was marked by intense thrust tectonics and crustal shortening during the Cenozoic (Fan et al., 1994). The northward displacement of the Pamir ultimately blocked or cut-off the connection between the Tarim Sea and the eastern branch of the Neotethys Ocean; this serves as an important factor that influenced the seawater retreat from different parts of the Tarim and Tajik Basins.

Significant indentation of the Pamir salient into Asia during the Cenozoic is also demonstrated by the large-scale strike-slip faults on the two flanks of the Pamir. In the eastern Pamir salient, the right-lateral Karakoram fault accommodates northward indentation of the Pamir Mountains (Sobel and Dumitru, 1997; Sobel et al., 2011) and the eastward lateral extrusion of the Tibetan plateau (Searle, 1996; Murphy et al., 2002). The offset is estimated to range from 200 km (Ratschbacher et al., 1994) to 400 to 600 km (Peltzer and Tapponnier, 1988; Schwab et al., 2004).

Many lines of evidence have indicated that middle to late Eocene tectonics in the Pamir was a response of the India-Eurasia collision that was initiated at ~55–50 Ma (Molnar and Tapponnier, 1975; Petterson and Windley, 1985; Beck et al., 1995; Rowley, 1996; Bignold and Treloar, 2003). Burtman and Molnar (1993) based their conclusion that separation of the North Pamir from the Western Kunlun Shan started in the late Eocene on regional stratigraphic data, which document both the retreat of a Late Cretaceous to Paleogene marine incursion in the composite Tajik-Tarim Basin, and the isolation of the Tajik Basin from the southwestern Tarim Basin.

Magmatism also provides evidence for the timing of tectonics. In the Pamir salient, the Indus Suture Zone limits the northern margin of the Indian Plate and the Kohistan-Ladakh arc (Fig. 1). During India's northward drift, Tethyan oceanic lithosphere was subducted northwards beneath the active Andean-type southern margin of Asia resulting in intrusion of the calcalkaline batholith along the Kohistan-Ladakh arc, which is sandwiched between the India Plate and the southern edge of Asia (the Karakoram terrane in the southern Pamir salient). I-type magmatism in the Ladakh Batholith continued until at least ~46 Ma (White et al., 2011). This might imply that the Indian Plate had not collided with the Kohistan-Ladakh arc by 46 Ma. St-Onge et al. (2010) proposed that the change in granite chemistry from an I-type granodiorite at ~57.7 Ma to emplacement of S-type leucocratic dykes at ~47 Ma at Ladakh marked the end of subduction-related plutonism. This accretion event related to the India–Asia collision is comparable to the timing of final marine sedimentation at ~50.5 Ma in Ladakh (Green et al., 2008), as well as to the crustal thickening in northern Tibet that had began prior to 46 Ma in the western Kunlun Shan thrust belt (Yin et al., 2002). Moreover, stratigraphic data favor closure of the ocean and terminal formation of the Indus Suture starting in the Late Ypresian (~50 Ma) (Rowley, 1996, 1998; Najman,

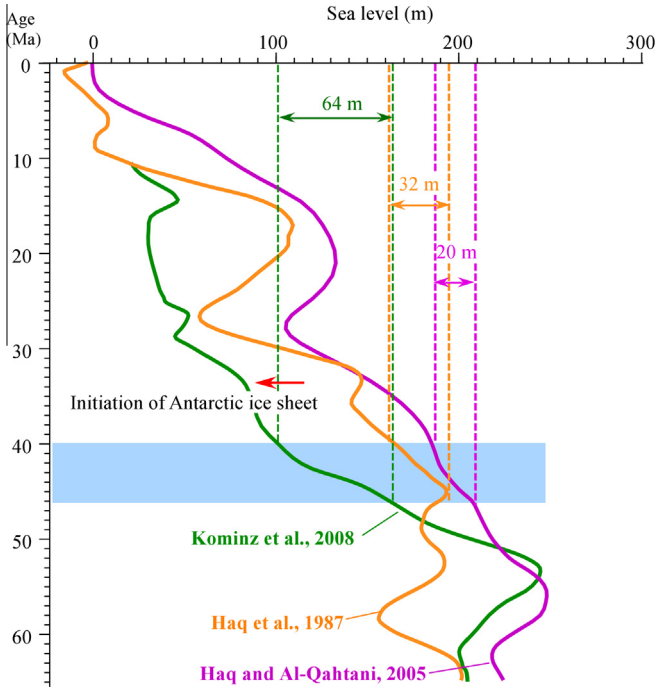

Fig. 10. Cenozoic global eustatic sea-level fluctuations (Haq et al., 1987; Haq and Al-Qahtani, 2005; Kominz et al., 2008). The estimated sea-level decreases ranging from 20 m to 64 m were based on different data sources during the time interval between 47 Ma and 40 Ma.

2006; Wu et al., 2014), which is also consistent with dating of detrital zircons from sandstones in the Indus suture zone (Wu et al., 2007; Henderson et al., 2011).

All the above evidence demonstrates that the large-scale northward indentation was initiated at ~50 Ma, and accordingly this northward displacement of the Pamir salient must have played an important role in controlling the sea water retreat from the southwestern margin of the Tarim Basin.

Moreover, the northward indentation and uplift of the Pamir-west Kunlun orogen favored the erosional denudation of the rising mountains and the deposition of the eroded materials in the Tarim Basin; these processes played a further role in the seawater retreat (Fig. 9b).

Additionally, the Cenozoic era was characterized by stepwise drying and cooling trends; one of the most prominent climate cooling events occurred across the Eocene–Oligocene transition at 34 Ma, marked by formation of the Antarctic ice sheet (Kennett, 1977; Miller et al., 1991; Zachos et al., 2001). However, this climatic cooling and thus eustatic sea level was later than the final sea water retreat from the southwestern margin of the Tarim Basin (Fig. 10). Although the sea level did decrease between 47 Ma and 40 Ma ranging from 64 m to 20 m according to different authors (Fig. 10), this was a limited sea-level decrease that cannot account for large scale seawater retreat from different parts of the Tarim Basin. In this context, climatic cooling only played a minor role.

6. Conclusions

The timing of the gradual seawater retreat from the southwestern margin of the Tarim Basin is a key for understanding the northward indentation of the Pamir syntaxis at the western end of the Himalayan–Tibetan orogen, it was also a key to understanding the climatic effects of the Neotethys Ocean on the aridification in the downwind Asian interior.

Our new magnetostratigraphic and biostratigraphic data provide a novel high-resolution time-scale for the Cenozoic strata in the northern foreland basin of the southwestern Kunlun orogen. Our results demonstrate that seawater retreat in the Keliyang section occurred at ~40 Ma, which was later than the early sea retreat of ~47 Ma at Oytag. In view of the differences in timing of Tarim Sea events, together with the other previous results, we propose a model of diachronous seawater retreat from the southwestern margin of the Tarim Basin in the late Eocene ranging from 47 Ma to 40 Ma. We also suggest that the northward indentation of the Pamir salient played an important role in controlling this diachronous seawater retreat, and that the eustatic sea-level changes related to global scale climatic cooling only played a minor role.

Acknowledgements

This work was supported by the “Strategic Priority Research Program” of the Chinese Academy of Science (XDB03020500), the National Basic Research Program of China (2013CB956400), and the National Nature Science Foundation of China (41290251 and 41272203). We thank Ma Yuanxu, Xue Guoliang, Xie Liqiang, and Tan Fei for their help in field sampling. We also thank Miguel Garcés and Maodu Yan for their valuable comments and suggestions that have substantially improved our manuscript.

References

Amidon, W.H., Hynek, S.A., 2010. Exhumational history of the north central Pamir. Tectonics 29, TC5017. http://dx.doi.org/10.1029/2009TC002589.

Beck, R.A., Burbank, D.W., Sercombe, W.J., Riley, G.W., Barndt, J.K., Berry, J.R., Afzal, J., Khan, A.M., Jurgen, H., Metje, J., Cheema, A., Shafique, N.A., Lawrence, R.D., Khan, M.A., 1995. Stratigraphic evidence for an early collision between northwest India and Asia. Nature 373, 55–58.

Bershaw, J., Garzione, C.N., Schoenbohm, L., Gehrels, G., Tao, L., 2012. Cenozoic evolution of the Pamir plateau based on stratigraphy, zircon provenance, and stable isotopes of foreland basin sediments at Oytag (Wuyitake) in the Tarim Basin (west China). J. Asian Earth Sci. 44, 136–148.

Bignold, S.M., Treloar, P.J., 2003. Northward subduction of the Indian plate beneath the Kohistan island arc, Pakistan Himalaya: new evidence from isotopic data. J. Geol. Soc. London 160, 377–384.

Bosboom, R.E., Dupont-Nivet, G., Houben, A.J.P., Brinkhuis, H., Villa, G., Mandic, O., Stoica, M., Zachariasse, W.J., Guo, Z., Li, C., Krijgsman, W., 2011. Late Eocene sea retreat from the Tarim Basin (West China) and concomitant Asian paleoenvironmental change. Palaeogeogr. Palaeoclimat. Palaeoecol. 299, 385–398.

Bosboom, R.E., Dupont-Nivet, G., Grothe, A., Brinkhuis, H., Villa, G., Mandic, O., Stoica, M., Huang, W., Yang, W., Guo, Z., Krijgsman, W., 2014a. Linking Tarim Basin sea retreat (West China) and Asian aridification in the late Eocene. Basin Res. 26, 621–640.

Bosboom, R.E., Dupont-Nivet, G., Grothe, A., Brinkhuis, H., Villa, G., Mandic, O., Stoica, M., Kouwenhoven, T., Huang, W., Yang, W., Guo, Z., 2014b. Timing, cause and impact of the late Eocene stepwise sea retreat from the Tarim Basin (West China). Palaeogeogr. Palaeoclimat. Palaeoecol. 403, 101–118.

Burtman, V.S., 2000. Cenozoic crustal shortening between the Pamir and Tien Shan and a reconstruction of the Pamir-Tien Shan transition zone for the Cretaceous and Palaeogene. Tectonophysics 319, 69–92.

Burtman, V.S., 2013. The geodynamics of the Pamir-Punjab syntaxis. Geotectonics 47, 31–51.

Burtman, V.S., Molnar, P., 1993. Geological and geophysical evidence for deep subduction of continental crust beneath the Pamir. Geol. Soc. Am. Spec. Pap. 281, 1–76.

Cande, S.C., Kent, D.V., 1995. Revised calibration of the geomagnetic polarity timescale for the Late Cretaceous and Cenozoic. J. Geophys. Res. 100, 6093–6095.

Cao, K., Bernet, M., Wang, G.C., van der Beek, P., Wang, A., Zhang, K.X., Enkelmann, E., 2013. Focused Pliocene–Quaternary exhumation of the Eastern Pamir domes, western China. Earth Planet. Sci. Lett. 363, 16–26.

Carrapa, B., DeCelles, P.G., Wang, X., Clementz, M.T., Mancin, N., Stoica, M., Kraatz, B., Meng, J., Abdulov, S., Chen, F.H., 2015. Tectono-climatic implications of Eocene Paratethys regression in the Tajik basin of central Asia. Earth Planet. Sci. Lett. 424, 168–178.

Chang, H., An, Z.S., Liu, W.G., Qiang, X.K., Song, Y.G., Ao, H., 2012. Magnetostratigraphic and paleoenvironmental records for a Late Cenozoic sedimentary sequence drilled from Lop Nor in the eastern Tarim Basin. Global Planet. Change 80–81, 113–122.

Cheng, X., Lei, G., Chen, H., Du, Z., Liao, L., Luo, J., Shi, J., 2011. Cenozoic structural deformation of the Fusha-Keliyang area in the piedmont of the western Kunlun Mountains and its control on hydrocarbon accumulation. Acta Petrol. Sin. 32, 83–89.

Collinson, D.W., 1983. Methods in Rock Magnetism and Palaeomagnetism: Techniques and Instruments. Chapman & Hall, London.

Cowgill, E., 2010. Cenozoic right-slip faulting along the eastern margin of the Pamir salient, northwestern China. Geol. Soc. Am. Bull. 122, 145–161.

Fan, G.W., Ni, J.F., Wallace, T.C., 1994. Active tectonics of the Pamirs and Karakorum. J. Geophys. Res. 99 (B4), 7131–7160.

Fisher, R.A., 1953. Dispersion on a sphere. Proc. R. Soc. London, Ser. A 217, 295–305.

Fu, B.H., Ninomiya, Y., Guo, J.M., 2010. Slip partitioning in the northeast Pamir-Tian Shan convergence zone. Tectonophysics 483, 344–364.

Green, O.R., Searle, M.P., Corfield, R.I., Corfield, R.M., 2008. Cretaceous–Tertiary carbonate platform evolution and the age of the India–Asia collision along the Ladakh Himalaya (Northwest India). J. Geol. 116, 331–353.

Guo, X.P., Ding, X.Z., 2002. New progress in the study of marine transgressional events and marine strata of the Meso-Cenozoic in the Tarim Basin. Acta Geol. Sin. 76, 299–307.

Haq, B.U., Al-Qahtani, A.M., 2005. Phanerozoic cycles of sea-level change on the Arabian Platform. GeoArabia 10, 127–160.

Haq, B.U., Hardenbol, J., Vail, P.R., 1987. Chronology of fluctuating sea levels since the Triassic (250 million years ago to present). Science 235, 1156–1167.

He, C.Q., 1991. Late Cretaceous–Early Tertiary Microphytoplankton from the Western Tarim Basin in Southwestern Xinjiang, China. Science Press, Beijing.

Henderson, A.L., Najman, Y., Parrish, R., Mark, D.F., Foster, G.L., 2011. Constraints to the timing of India-Eurasia collision; a re-evaluation of evidence from the Indus Basin sedimentary rocks of the Indus-Tsangpo Suture Zone, Ladakh, India. Earth Sci. Rev. 106, 265–292.

Jin, X., Wang, J., Chen, B., Ren, L., 2003. Cenozoic depositional sequences in the piedmont of the west Kunlun and their paleogeographic and tectonic implications. J. Asian Earth Sci. 21, 755–765.

Kennett, J.P., 1977. Cenozoic evolution of Antarctic glaciation, the circum-Antarctic Ocean, and their impact on global paleoceanography. J. Geophys. Res. 82, 3843–3859.

Kirschvink, J., 1980. The least square line and the analysis of paleomagnetic data. Geophys. J. R. Astron. Soc. 62, 699–718.

Kominz, M.A., Browning, J.V., Miller, K.G., Sugarman, P.J., Mizintseva, S., Scotese, C.R., 2008. Late Cretaceous to Miocene sea-level estimates from the New Jersey and Delaware coastal plain boreholes: an error analysis. Basin Res. 20, 211–226.

Lan, X., Wei, J.M., 1995. Late Cretaceous–Early Tertiary Marine Bivalve Fauna from the Western Tarim Basin. Science Press, Beijing.

Li, D., Liang, D., Jia, C., Wang, G., Wu, Q., He, D., 1996. Hydrocarbon accumulations in the Tarim Basin, China. AAPG Bull. 80, 1587–1603.

Liu, W., Liu, Z., An, Z., Sun, J., Chang, H., Wang, N., Dong, J., Wang, H., 2014. Late Miocene episodic lakes in the arid Tarim Basin, western China. Proc. Natl. Acad. Sci. USA 111, 16292–16296.
McFadden, P.L., McElhinny, M.W., 1990. Classification of the reversal test in paleomagnetism. Geophys. J. Int. 103, 725–729.
Miller, K.G., Wright, J.D., Fairbanks, R.G., 1991. Unlocking the icehouse: Oligocene–Miocene oxygen isotopes, eustasy, and margin erosion. J. Geophys. Res. 96, 6829–6848.
Molnar, P., Tapponnier, P., 1975. Cenozoic tectonics of Asia: effects of a continental collision. Science 189, 419–426.
Murphy, M.A., Yin, A., Kapp, P., Harrison, T.M., Manning, C.E., 2002. Structural and thermal evolution of the Gurla Mandhata metamorphic core complex, southwest Tibet. Geol. Soc. Am. Bull. 114, 428–447.
Najman, Y., 2006. The detrital record of orogenesis: a review of approaches and techniques used in the Himalayan sedimentary basins. Earth Sci. Rev. 74, 1–72.
Negredo, A.M., Replumaz, A., Villasenor, A., Guillot, S., 2007. Modeling the evolution of continental subduction process in the Pamir-Hindu Kush region. Earth Planet. Sci. Lett. 259, 212–225.
Pan, H.Z., Yang, S.Q., Sun, D.L., 1991. Late Cretaceous–Early Tertiary Gastropods, Sea Urchin, and Brachiopod from the Western Tarim Basin in Southwestern Xinjiang, China. Science Press, Beijing.
Peltzer, G., Tapponnier, P., 1988. Formation and evolution of strike-slip faults, rifts, and basins during the India–Asia collision: an experimental approach. J. Geophys. Res. 93, 15085–15117.
Petterson, M.G., Windley, B.F., 1985. Rb–Sr dating of the Kohistan arc batholith in the Trans-Himalaya of N. Pakistan and tectonic implications. Earth Planet. Sci. Lett. 74, 45–75.
Piller, W.E., Harzhauser, M., Mandic, O., 2007. Miocene Central Paratethys stratigraphy – current status and future directions. Stratigraphy 4, 151–168.
Popov, S.V., Rogl, F., Rozanov, A.Y., Steininger, F.F., Shcherba, I.G., Kovac, M., 2004. Lithological-Paleogeographic maps of Paratethys 10 Maps Late Eocene to Pliocene. Cour. Forsch.-Inst. Senckenberg 250, 1–46.
Popov, S.V., Shcherba, I.G., Ilyina, L.B., Nevesskaya, L.A., Paramonova, N.P., Khondkarian, S.O., Magyar, I., 2006. Late Miocene to Pliocene palaeogeography of the Paratethys and itsrelation to the Mediterranean. Palaeogeogr. Palaeoclimat. Palaeoecol. 238, 91–106.
Ratschbacher, L., Frisch, W., Herrman, U., Strecker, M., 1994. Distributed deformation in Southern and Western Tibet during and after the India–Asia collision. J. Geophys. Res. 99, 19817–19945.
Replumaz, A., Guillot, S., Villaseñor, A., Negredo, A.M., 2013. Amount of Asian lithospheric mantle subducted during the India/Asia collision. Gondwana Res. 24, 936–945.
Replumaz, A., Capitanio, F.A., Guillot, S., Negredo, A.M., Villaseñor, A., 2014. The coupling of Indian subduction and Asian continental tectonics. Gondwana Res. 26, 608–626.
Ritts, B., Yue, Y., Graham, S., Sobel, E., Abbink, O.A., Stockli, D., 2008. From sea level to high elevation in 15 million years. Am. J. Sci. 308, 657–678.
Robinson, A.C., Yin, A., Manning, C.E., Harrison, T.M., Zhang, S.H., Wang, X.F., 2004. Tectonic evolution of the northeastern Pamir: constraints from the northern portion of the Cenozoic Kongur Shan extensional system, western China. Geol. Soc. Am. Bull. 116, 953–973.
Robinson, A.C., Yin, A., Manning, C.E., Harrison, T.M., Zhang, S.H., Wang, X.F., 2007. Cenozoic evolution of the eastern Pamir: implications for strain-accommodation mechanisms at the western end of the Himalayan-Tibetan orogen. Geol. Soc. Am. Bull. 119, 882–896.
Robinson, A.C., Ducea, M., Lapen, T.J., 2012. Detrital zircon and isotopic constraints on the crustal architecture and tectonic evolution of the northeastern Pamir. Tectonics 31, TC2016. http://dx.doi.org/10.1029/2011TC003013.
Rögl, F., 1999. Mediterranean and Paratethys facts and hypotheses of an Oligocene to Miocene paleogeography (short overview). Geol. Carpath. 50, 339–349.
Rowley, D.B., 1996. Age of collision between India and Asia: a review of the stratigraphic data. Earth Planet. Sci. Lett. 145, 1–13.
Rowley, D.B., 1998. Minimum age of initiation of collision between India and Asia north of Everest based on the subsidence history of the Zhepure Mountain section. J. Geol. 106, 229–235.
Schulz, H.M., Bechtel, A., Sachsenhofer, R.F., 2005. The birth of the Paratethys during the Early Oligocene: from Tethys to an ancient Black Sea analogue? Global Planet. Change 49, 163–176.
Schwab, M., Ratschbacher, L., Siebel, W., McWilliams, M., Minaev, V., Lutkov, V., Chen, F., Stanek, K., Nelson, B., Frisch, W., Wooden, J.L., 2004. Assembly of the Pamirs: age and origin of magmatic belts from the southern Tien Shan to the southern Pamirs and their relation to Tibet. Tectonics 23, TC4002. http://dx.doi.org/10.1029/2003TC001583.
Searle, M.P., 1996. Geological evidence against large scale pre-holocene offsets along the Karakoram fault: implications for the limited extrusion of the Tibetan Plateau. Tectonics 15, 171–186. http://dx.doi.org/10.1029/95TC01693.
Searle, M.P., 2011. Geological evolution of the Karakoram Ranges. Ital. J. Geosci. 130, 147–159.
Searle, M.P., Khan, M.A., Fraser, J.E., Gough, S.J., 1999. The tectonic evolution of the Kohistan-Karakoram collision belt along the Karakoram Highway transect, north Pakistan. Tectonics 18, 929–949.
Sobel, E.R., Dumitru, T.A., 1997. Thrusting and exhumation around the margins of the western Tarim basin during the India–Asia collision. J. Geophys. Res. 102 (B3), 5043–5063.
Sobel, E.R., Schoenbohm, L.M., Chen, J., Thiede, R., Stockli, D.F., Sudo, M., Strecker, M. R., 2011. Late Miocene–Pliocene deceleration of dextral slip between Pamir and Tarim: implications for Pamir orogenesis. Earth Planet. Sci. Lett. 304, 369–378.
St-Onge, M.R., Rayner, N., Searle, M.P., 2010. Zircon age determinations for the Ladakh batholith at Chumathang (Northwest India): implications for the age of the India–Asia collision in the Ladakh Himalaya. Tectonophysics 495, 171–183.
Sun, J.M., Jiang, M.S., 2013. Eocene seawater retreat from the southwest Tarim Basin and implications for early Cenozoic tectonic evolution in the Pamir Plateau. Tectonophysics 588, 27–38.
Sun, J.M., Liu, T.S., 2006. The age of the Taklimakan Desert. Science 312, 1621.
Sun, J.M., Alloway, B., Fang, X.M., Windley, B.F., 2015. Refuting the evidence for an earlier birth of the Taklimakan Desert. Proc. Natl. Acad. Sci. USA 112, E5556–E5557.
Tapponnier, P., Molnar, P., 1979. Active faulting and Cenozoic tectonics of the Tien Shan, Mongolia and Baykal regions. J. Geophys. Res. 84 (B7), 3425–3459.
Tapponnier, P., Xu, Z.Q., Roger, F., Meyer, B., Arnaud, N., Wittlinger, G., Yang, J.S., 2001. Oblique stepwise rise and growth of the Tibet Plateau. Science 294, 1671–1677.
Thiede, R.C., Sobel, E., Chen, J., Schoenbohm, L.M., Stockli, D.F., Sudo, M., Strecker, M. R., 2013. Late Cenozoic extension and crustal doming in the India-Eurasia collision zone: new thermochronologic constraints from the NE Chinese Pamir. Tectonics 32, 763–779. http://dx.doi.org/10.1002/tect/20050.
Thompson, J.A., Burbank, D.W., Li, T., Chen, J., Bookhagen, B., 2015. Late Miocene northward propagation of the northeast Pamir thrust system, northwest China. Tectonics 34. http://dx.doi.org/10.1002/2014TC003690.
Vasiliev, I., Krijgsman, W., Langereis, C.G., Panaiotu, C.E., Matenco, L., Bertotti, G., 2004. Towards an astrochronological framework for the eastern Paratethys Mio-Pliocene sedimentary sequences of the FocYani basin (Romania). Earth Planet. Sci. Lett. 227, 231–247.
Waldhör, M., Appel, E., Frisch, W., Patzelt, A., 2001. Palaeomagnetic investigation in the Pamirs and its tectonic implications. J. Asian Earth Sci. 19, 429–451.
Wang, E., Wan, J.L., Liu, J.Q., 2003. Late Cenozoic geological evolution of the foreland basin bordering the West Kunlun range in Pulu area: constraints on timing of uplift of northern margin of the Tibetan Plateau. J. Geophys. Res. 108 (B8), 2401. http://dx.doi.org/10.1029/2002JB001877.
Wang, X., Sun, D.H., Chen, F.H., Wang, F., Li, B.F., Popov, S.V., Wu, S., Zhang, Y.B., Li, Z. J., 2014. Cenozoic paleo-environmental evolution of the Pamir-Tien Shan convergence zone. J. Asian Earth Sci. 80, 84–100.
White, L.T., Ahmed, T., Ireland, T.R., Lister, G.S., Forster, M.A., 2011. Deconvolving episodic age spectra from zircons of the Ladakh batholith, northwest Indian Himalaya. Chem. Geol. 289, 179–196.
Wu, F.Y., Clift, P.D., Yang, J.H., 2007. Zircon Hf isotopic constraints on the sources of the Indus Molasse, Ladakh Himalaya, India. Tectonics 26, TC2014. http://dx.doi.org/10.1029/2006TC002051.
Wu, F.Y., Ji, W.Q., Wang, J.G., Liu, C.Z., Chung, S.L., Clift, P., 2014. Zircon U–Pb and Hf isotopic constraints on the onset time of India–Asia collision. Am. J. Sci. 314, 548–579.
Xiao, W.J., Han, F., Windley, B.F., Yuan, C., Zhou, H., Li, J.L., 2003. Multiple accretionary orogenesis and episodic growth of continents: insights from the Western Kunlun Range, Central Asia. Int. Geol. Rev. 45, 303–328.
Xiao, W.J., Windley, B.F., Liu, D.Y., Jian, P., Liu, C.Z., Yuan, C., Sun, M., 2005. Accretionary tectonics of the Western Kunlun orogen, China: a Paleozoic-early Mesozoic, long-lived active continental margin with implications for the growth of southern Eurasia. J. Geol. 113, 687–705.
Yang, H.R., Jiang, X.T., Lin, S.P., 1995. Late Cretaceous–Early Tertiary Ostracods from the Western Tarim Basin in Southwestern Xinjiang, China. Science Press, Beijing.
Yin, A., Harrison, T.M., 2000. Geologic evolution of the Himalayan-Tibetan orogen. Annu. Rev. Earth Planet. Sci. 28, 211–280.
Yin, A., Rumelhart, P.E., Butler, R., Cowgill, E., Harrison, T.M., Foster, D.A., Ingersoll, R. V., Zhang, Q., Zhou, X., Wang, X., Hanson, A., Raza, A., 2002. Tectonic history of the Altyn Tagh fault system in northern Tibet inferred from Cenozoic sedimentation. Geol. Soc. Am. Bull. 114, 1257–1295.
Zachos, J.C., Pagani, M., Sloan, L., Thomas, E., Billups, K., 2001. Trends, rhythms, and aberrations in global climate 65 Ma to present. Science 292, 686–693.
Zhong, S.L., 1992. Late Cretaceous–Early Tertiary Calcareous Nannofossils from the Western Tarim Basin in Southwestern Xinjiang, China. Science Press, Beijing.